Electronic Materials Letters, Vol. 9, No. 3 (2013), pp. 299-307
DOI: 10.1007/s13391-013-2243-y

Using a Functional Epoxy, Micron Silver Flakes, Nano Silver Spheres, and Treated Single-Wall Carbon Nanotubes to Prepare High Performance Electrically Conductive Adhesives

Hui-Wang Cui,[1,2,*] Dong-Sheng Li,[1] and Qiong Fan[1]

[1]Key State Laboratory for New Displays & System Applications and SMIT Center, College of Automation and Mechanical Engineering, Shanghai University, Shanghai 200072, China
[2]Institute of Scientific and Industrial Research, Osaka University, 565-0871, Osaka, Japan

(received date: 14 December 2012 / accepted date: 18 January 2013 / published date: 10 May 2013)

In this study, a matrix resin containing a functional epoxy, a reactive diluent, a silane-coupling agent, and a curing agent was used to fabricate three modal electrically conductive adhesives (ECAs) with micron silver flakes, nano silver spheres, and treated single-wall carbon nanotubes (CNT). Results showed that too many micron silver flakes reduced the bulk resistivity and adhesion strength of uni-modal ECAs (matrix resin and micron silver flakes). As the nano silver spheres increased, the bulk resistivity of bi-modal ECAs (matrix resin, micron silver flakes, and nano silver spheres) firstly decreased, and then increased again. The adhesion strength decreased also. The bulk resistivity and adhesion strength of tri-modal ECAs (matrix resin, micron silver flakes, nano silver spheres, and treated CNT) both were reduced by the treated CNT greatly. These ECAs could be cured at 120°C or any higher temperature than this with different curing time. They all had high temperature stability with a pyrolysis temperature above 350°C and a glass transition temperature around 180°C.

Keywords: conductive adhesives, nanoparticles, electronic package

1. INTRODUCTION

Connecting materials play an important role in the electronic package. Their properties affect the value and application of electronic products directly. They should meet the requirements of micronized connection and connection strength for the electronic products. Meanwhile, some new demands for the development of connecting materials have been required by the environmental awareness. Therefore, researching and developing the low energy consumption, environmentally friendly, new connecting materials have become an inevitable development trend to replace the high-energy consumption, environmentally harmfully, traditional connecting materials. At present, Pb-Sn solder is a traditional connecting material. It has been used in the electrical, appliance, energy, and automotive and other fields widely. The general properties of Pb-Sn solder are good, but it does not work effectively in ultra- or micronized connection. In addition, it has poor creep resistance and the connection often needs high temperature. These defects limit the application of Pb-Sn solder seriously.

Electrically conductive adhesives (ECAs) avoid these defects to some extent.[1,2] ECAs have been developed greatly as the polymer technology flourishes. Their formulation,[3-5] reliability,[6,7] and mechanical and electrical properties[8-10] are mainly studied. However, ECAs also have some shortcomings, such as low electrical conductivity, low high temperature resistance, long curing time, etc.. To solve these problems, many efforts have been put on ECAs' reliability,[11-15] moisture absorption,[16] simulation,[17,18] fillers,[19-24] electricity,[12-15,21-25] and thermal properties.[12-15,21-28] In this study, a matrix resin containing a functional epoxy (main resin), a reactive diluent, a silane-coupling agent, and a curing agent was fixed with no solvent for solvent-free ECAs. Then three modal ECAs: uni-modal ECAs (matrix resin and micron silver flakes), bi-modal ECAs (matrix resin, micron silver flakes, and nano silver spheres), and tri-modal ECAs (matrix resin, micron silver flakes, nano silver spheres, and treated single-wall carbon nanotubes (CNT)), were fabricated to optimize the formulation. Their bulk resistivity, adhesion strength, and thermal properties were mainly studied in hope of providing optimized formulation and fabrication for ECAs that with low bulk resistivity, good adhesion strength, and high temperature stability.

2. EXPERIMENTAL PROCEDURE

2.1 Samples

The matrix resin contained a functional epoxy (N, N-

*Corresponding author: cuihuiwang@hotmail.com

diglycidyl-4-glycidyloxyaniline, Sigma-Aldrich, USA) as the main resin, a reactive diluent (2-ethylhexyl glycidyl ether, Sigma-Aldrich, USA), a silane-coupling agent (3-glycidoxypropyltrimethoxysilane, Sigma-Aldrich, USA), and a curing agent (1-cyanoethyl-2-ethyl-4-methylimidazole, Shikoku Chemicals, Japan). Three different modal ECAs: uni-modal ECAs (matrix resin and micron silver flakes), bi-modal ECAs (matrix resin, micron silver flakes, and nano silver spheres), and tri-modal ECAs (matrix resin, micron silver flakes, nano silver spheres, and treated CNT), were fabricated according to the different electrically conductive fillers. To treat CNT, 500 mg of CNT were immersed in the mixture of 30 mL of 98% sulfuric acid and 10 mL of 68% nitric acid at 50°C for 3 h, they were stirred by hand once every 30 min during the immersion, and then the treated CNT were washed, filtered, and dried at 100°C in a vacuum oven until the weight got constant. The size of micron silver flakes was 3 - 10 μm and their thickness was about 0.5 μm (Fukuda Metal Foil & Powder, Japan), the diameter of nano silver spheres was 500 - 1000 nm (Alfa Aesea, USA), and the outer diameter and length of CNT were 20 - 40 nm and 5 - 20 μm respectively (Applied Nono-Technologies, USA). To fabricate these ECAs, the matrix resin was firstly prepared. The functional epoxy, reactive diluent, silane-coupling agent, and curing agent were mixed together using a 78-1 magnetic mixer (Lantian, Hangzhou, China) until they became homogeneous. Subsequently, the electrically conductive fillers were incorporated into the matrix resin using a MIX500D SLOPE solder cream mixer (Smtech, Shenzhen, China) with a mixing speed of 3000 - 4000 rpm and a mixing time of 10 - 20 min. ECAs were then obtained, as shown in Table 1, Table 2, Table 3, and Fig. 1. In the fabrication, solvents were not added because air voids were often formed by the evaporation. After the fabrication, these ECAs were stored at –20°C. When tested, they were taken out to room temperature, thawed for 30 min, and stirred strongly by hand for about 5 - 10 min to make sure the electrically conductive fillers were distributed more evenly.

Table 1. Design of uni-modal ECAs.

Matrix Resin (vol. %)	Micron Ag (vol. %)
65	35
64	36
63	37
62	38
61	39

Table 2. Design of bi-modal ECAs.

Matrix Resin (vol. %)	Micron Ag (vol. %)	Nano Ag (vol. %)
62	37	1
62	36	2
62	35	3
62	34	4
62	33	5

Table 3. Design of tri-modal ECAs.

Matrix Resin (vol. %)	Micron Ag (vol. %)	Nano Ag (vol. %)	Treated CNT (vol. %)
62	36.9	1	0.1
62	36.8	1	0.2
62	36.7	1	0.3
62	36.6	1	0.4
62	36.5	1	0.5

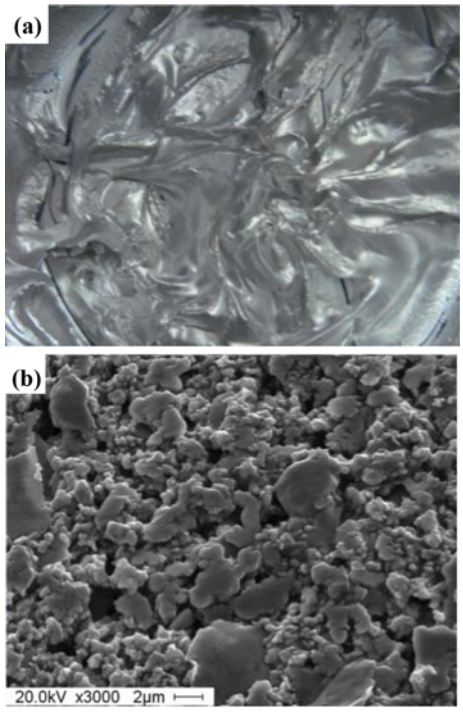

Fig. 1. ECAs samples: (a) liquid ECAs and (b) SEM image of bi-modal ECAs (33 vol. % micron Ag and 5 vol. % nano Ag).

2.2 Characterization

The curing of liquid ECAs samples were obtained using a Perkin Elmer Pyris 1 differential scanning calorimetry (DSC) (Perkin Elmer Inc., USA) heating from 50°C to 300°C at a rate of 5°C·min^{-1} and scanning in pure nitrogen atmosphere with a flow rate of 20 mL·min^{-1}. After cured at 150°C for 30 min and cooled to room temperature in a oven, the thermal stability of solid ECAs samples were investigated using a Perkin Elmer Pyris 1 thermogravimetric analysis (TGA) (Perkin Elmer Inc., USA) heating from 50°C to 900°C at a rate of 20°C·min^{-1} and scanning in pure nitrogen atmosphere with a flow rate of 20 mL·min^{-1}. Using a small scraper, liquid ECAs were manually flatly printed in a rectangle duct-like mold (50 mm × 5 mm × 0.5 mm) formed

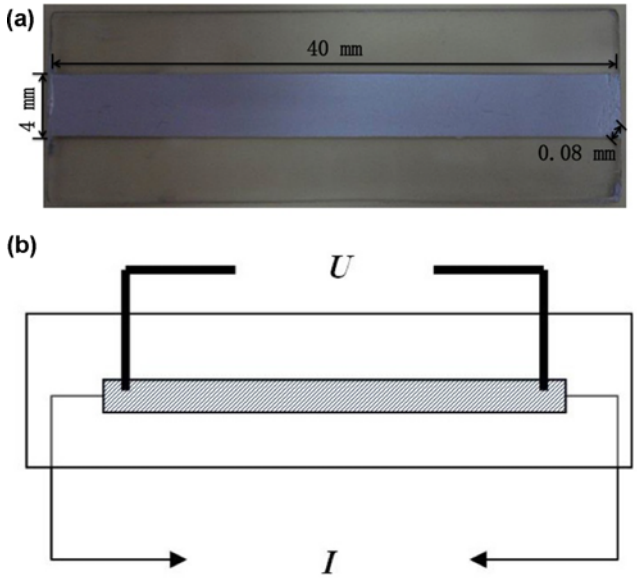

Fig. 2. Test method for bulk resistivity: (a) tested sample and (b) four-probe method.

by polytetrafluoroethene tape attached onto a glass substrate. After cured at 150°C for 30 min and cooled to room temperature in a oven, the ECAs films (Fig. 7(c)) obtained in the mold were tested using a Perkin Elmer 7e dynamic mechanical analysis (DMA) (Perkin Elmer Inc., USA) through three-point bending mode with a loading vibration frequency of 1 Hz and heating from 30°C to 300°C at a rate of 5°C·min^{-1}. Also using a small scraper, liquid ECAs were manually flatly printed onto a glass substrate to form stripes (40 mm × 4 mm × 0.08 mm). After cured at 150°C for 30 min and cooled to room temperature in a oven, the stripes (Fig. 2(a)) were tested through four-probe method using a Hewlett & Packard HP-34401A (HP, USA) to measure the voltage (U) and a Agilent E3631A Triple Output DC Power Supply (HP, USA) to measure the supply current (I). The test pattern is shown in Fig. 2(b). 6 sets of samples were tested. The bulk resistivity was calculated by:

$$\rho = \frac{U \times W \times H}{I \times L}.$$

Where ρ (Ω·cm) is the bulk resistivity, U (V) is the voltage, I (A) is the supply current, W (cm), H (cm), and L (cm) are the width, thickness, and length of the ECAs stripes respectively. The tested samples for adhesion strength were prepared according to Fig. 3(a). A copper metallization pad (diameter 2 mm, thickness 0.15 mm) on a FR4 printed circuit board substrate (40 mm × 12.5 mm × 2 mm) is used to determine the location of ECAs which would provide adhesion strength and also to mimic the practical application. After cured at 150°C for 30 min and cooled to room temperature in a oven, the samples were tested using a Instron 5548 Microtester (Instron, USA) according to Fig. 3(b) and (c) under a tensile rate of 10^{-3}·s^{-1}. 25 sets of samples were tested. The adhesion strength was calculated by:

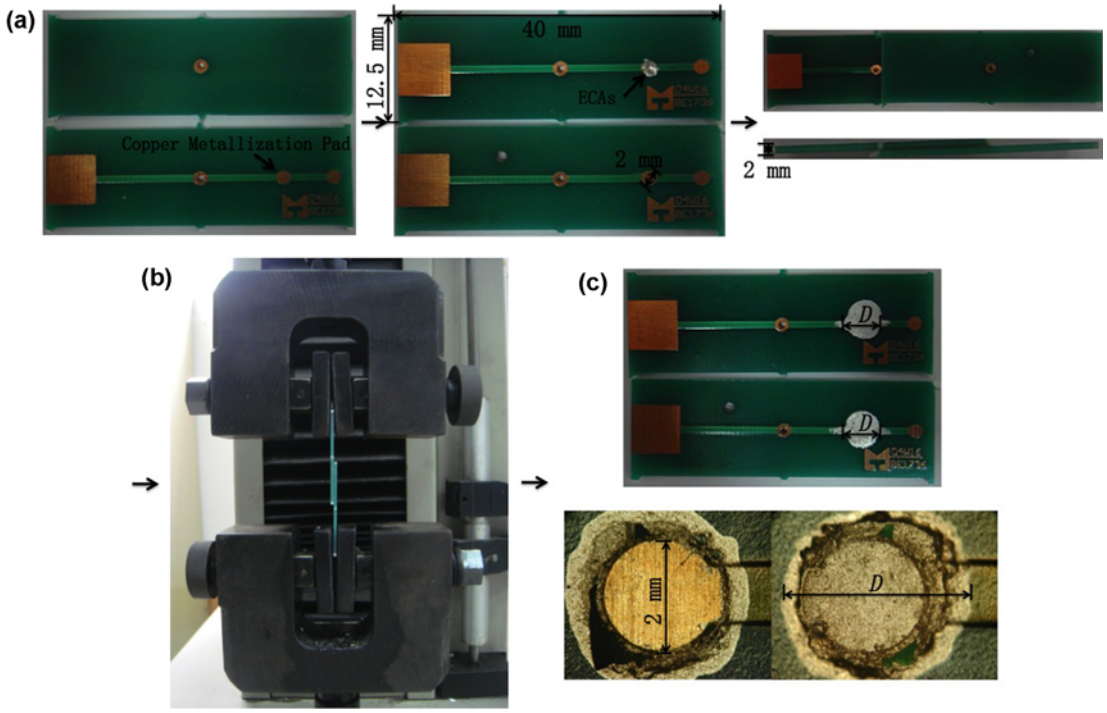

Fig. 3. Test method for adhesion strength: (a) preparation of tested samples, (b) adhesion strength test, and (c) fracture morphology of tested samples.

$$\sigma = \frac{F}{\pi \times \frac{D^2}{4}}.$$

Where σ (MPa) is the adhesion strength, F (N) is the maximum load, and D (mm) is the diameter of fracture cross-section region of ECAs joint. The dispersion of un- and treated CNT in acetone was observed using a JEOL JEM-200CX transmission electron microscopy (TEM) (JEOL, Japan). The solid samples of un- and treated CNT were scanned using a Nicolet AVATAR 370 Fourier transform infrared spectrometer (FTIR) (NICOLET, USA). The liquid ECAs samples and the fracture morphology of ECAs after adhesion tests were observed using a Camscan Apollo 300 scanning electron microscopy (SEM) (Camscan, UK).

3. RESULTS AND DISCUSSION

3.1 Uni-modal ECAs

As Table 1 shows, the bulk resistivity of uni-modal ECAs was related to the micron silver flake content closely. The contact or stack between/among micron silver flakes formed

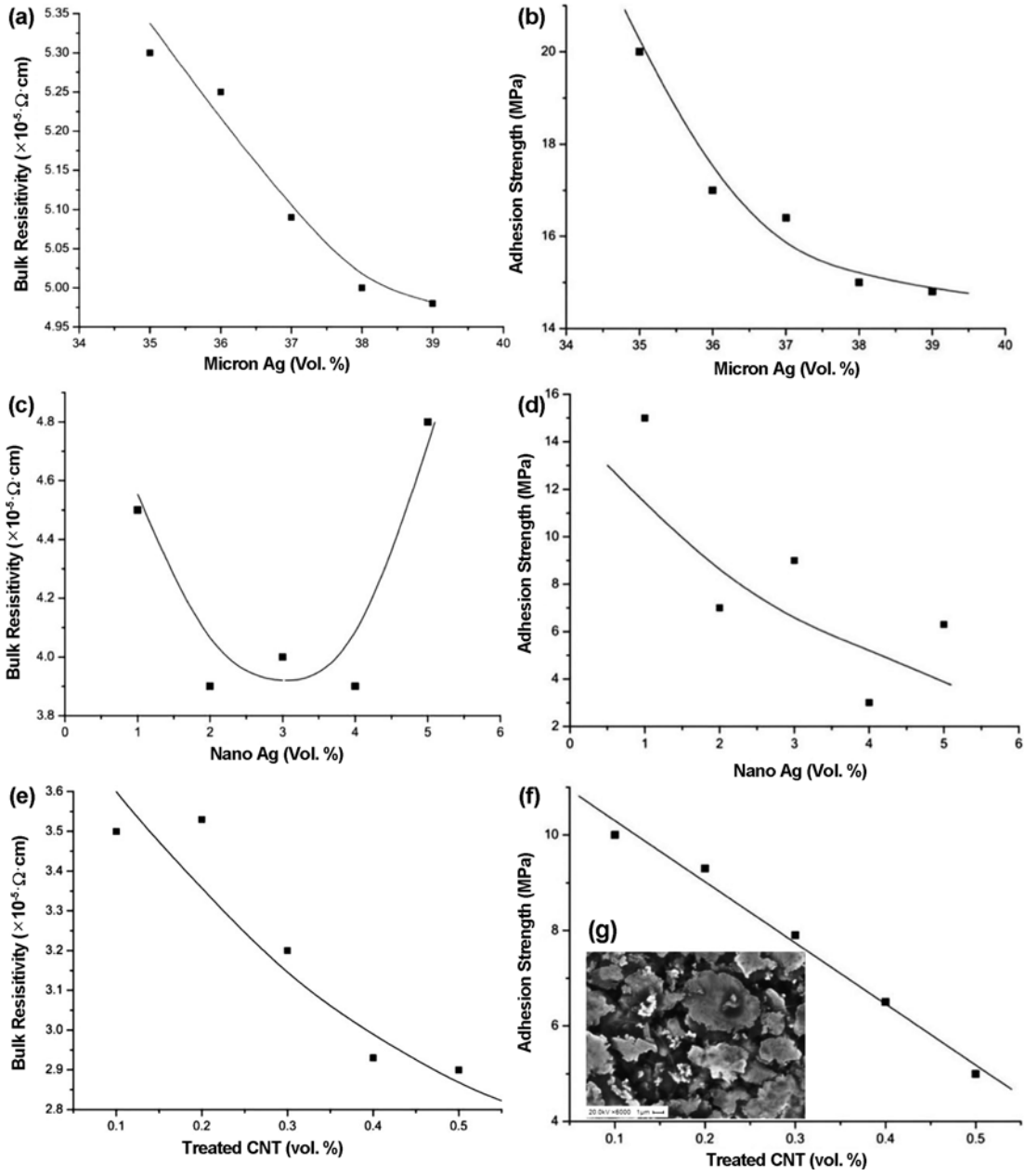

Fig. 4. Bulk resistivity of (a) uni-modal ECAs, (c) bi-modal ECAs, and (e) tri-modal ECAs, and adhesion strength of (b) uni-modal ECAs, (d) bi-modal ECAs, and (f) tri-modal ECAs, and (g) fracture morphology of tri-modal ECAs after adhesion test.

the electrically conductive channels. The more the micron silver flakes, the more the contact or stack between/among them, and therefore, the lower the bulk resistivity and the higher the electrical conductivity. As Figure 4(a) shows, the bulk resistivity decreased with the increase of micron silver flakes. When the micron silver flake content exceeded a certain amount of 38 vol. %, the bulk resistivity decreased slowly. In other words, the appropriate micron silver flake content was 38 vol. % for uni-modal ECAs, and the bulk resistivity was as low as 5.0×10^{-5} Ω·cm at this point.

The properties of epoxy and the electrically conductive fillers affect the adhesion strength of ECAs significantly.[29,30] In un-modal ECAs, with the increase of micron silver flakes, the epoxy between/among them decreased that did not form continuous film. The more the micron silver flakes, the worse the adhesion between epoxy and substrate, and thus the lower the adhesion strength. Too many micron silver flakes had negative or bad effect on the adhesion properties of ECAs, as shown in Fig. 4(b). The adhesion strength was 15.2 MPa at 38 vol. % of the micron silver flake content.

3.2 Bi-modal ECAs

Micron silver flakes are always used as the main electrically conductive fillers for traditional ECAs, but the bulk resistivity is too high which often limits the application in many fields. Nano technology has provided a possible solution to this problem. At some extent, some similar applications have appeared, such as nano silver spheres, CNT and so on. On one hand, nano silver spheres can fill the gap between/among micron silver flakes when they are used together. The contact or stack between/among them increases, which is very helpful to form electrically conductive channels and improve the electrical conductivity. On the other hand, the macroscopic properties of nano silver spheres are affected by their size and morphology directly, so their physical and chemical properties can be adjusted easily by controlling the size and morphology.[31-34]

On the basis of un-modal ECAs, the bi-modal ECAs were designed (Table 2). The total electrically conductive filler content was 38 vol. %. As Figure 4(c) shows, the bulk resistivity of bi-modal ECAs decreased with the increase of nano silver spheres. The lowest bulk resistivity was 3.9×10^{-5} Ω·cm at 3 vol. % of nano silver spheres. After this point, increasing the nano silver sphere content did not continue to lower the bulk resistivity, oppositely, it caused the bulk resistivity increasing. In the design of bi-modal ECAs, the total electrically conductive filler content was fixed at 38 vol. %, so increasing nano silver sphere content meant decreasing micron silver flake content. This change reduced the electrically conductive channels formed by micron silver flakes. Some nano silver spheres filled the gap between/among micron silver flakes, which did not contact to each other originally. Other nano silver spheres filled the space resulted from the decrease of micron silver flakes. At the beginning, a few micron silver flakes were replaced by some nano silver spheres and the contact or stack between/among them increased with the increase of nano silver spheres to lead to more electrically conductive channels, so the bulk resistivity decreased and the electrical conductivity increased. As more and more nano silver spheres were added, they embedded in the gap or space between/among micron silver flakes fully and completely. The formation of electrically conductive channels was improved greatly to obtain lower bulk resistivity of 3.9×10^{-5} - 4.0×10^{-5} Ω·cm at 2 vol. %-4 vol. % of the nano silver sphere content. Exceeding these points, especially exceeding 3 vol. % of nano silver spheres, the bulk resistivity did not continue to decrease but showed a increasing. This is because too many nano silver spheres were added and too many micron silver flakes were reduced. Nano silver spheres filled the gap between/among micron silver flakes and the space resulted from the decrease of micron silver flakes, but this had more negative effect than positive effect. On one hand, the contact or stack between/among micron silver flakes decreased greatly. On the other hand, the nano silver spheres distributed loosely in a large space, and might get agglomeration partially, so they could not well replace the close contact or stack and the electrically conductive channels formed by micron silver flakes with a same volume. Therefore, the increase of electrically conductive channels caused by the increase of nano silver spheres could not make up the decrease of electrically conductive channels caused by the decrease of micron silver flakes. The bulk resistivity increased again.

The variation of adhesion strength for bi-modal ECAs was similar to that of uni-modal ECAs. It decreased with the increase of nano silver spheres, as shown in Fig. 4(d). Nano silver spheres affected the adhesion strength directly. The maximum adhesion strength was 15 MPa at 1 vol. % of nano silver spheres, which was slightly lower than the uni-modal ECAs at 15.2 MPa at 38 vol. % of micron silver flakes. The minimum adhesion strength only was 2.8 MPa at 4 vol. % of nano silver spheres. The decrement was very significant. For bi-modal ECAs, adding nano silver spheres to replace some micron silver flakes might be the reason that caused the decrease of adhesion strength. This coincided with the solid-to-solid contact point theory.[35] Uni-modal ECAs only had micron silver flakes, so had few solid-to-solid contact points. In bi-modal ECAs, however, solid-to-solid contact points increased sharply because of nano silver spheres, to reduce the adhesion strength. Here, the bulk resistivity and adhesion strength were 4.5×10^{-5} Ω·cm and 15 MPa, respectively, for bi-modal ECAs at 37 vol. % of micron silver flakes and 1 vol. % of nano silver spheres.

3.3 Tri-modal ECAs

CNT or CNT plated by silver can be used as electrically

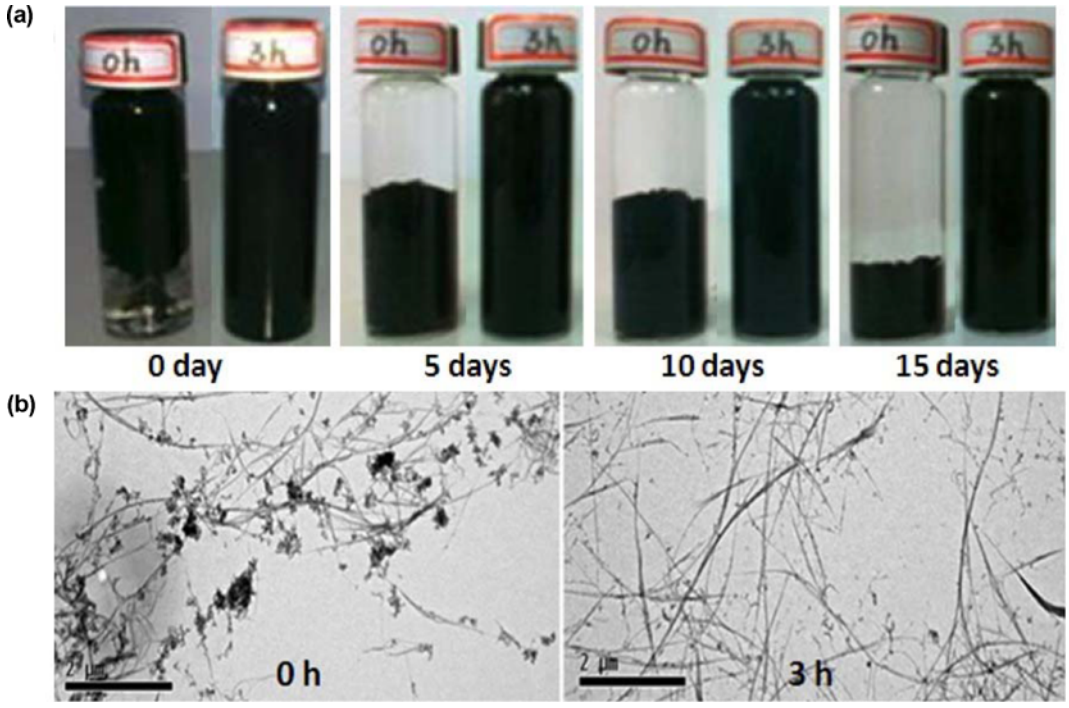

Fig. 5. (a) dispersion of un-treated CNT and treated CNT in acetone and (b) their TEM images.

conductive filler to contribute fully to the formation of nano fiber networks and nano fiber structures. These networks or structures are very helpful for the formation of electrically conductive channels in ECAs.[36,37] As a linear structural material, CNT can connect silver particles easily to form electrically conductive networks to improve the electrical conductivity. However, the compatibility between CNT and epoxy is so poor that CNT cannot disperse in epoxy uniformly and its content cannot be increased, either. Therefore, the surface of CNT should be treated before used in ECAs. CNT surface usually has some micro defects. Treated by concentrated nitric acid or sulfuric acid, the acid molecules react with CNT, and some active groups including polymeric and polar groups are connected to these defects to improve the compatibly with epoxy.[38,39] In this study, CNT was treated by a mixture of sulfuric acid and nitric acid at 50°C for 3 h. During the treatment, un- and treated CNT were dispersed in acetone by ultrasonic. As Figure 5(a) shows, un-treated CNT delaminated and deposited to show poor dispersion. Oppositely, the dispersion of treated CNT was good. Even after stood for 15 days, it still dispersed well in acetone. Observed by TEM, un-treated CNT had some agglomeration, while treated-CNT not, as shown in Fig. 5(b). As Figure 6(a) and (b) shows, the structure of CNT also changed: the wide transmittance peaks of symmetrical stretching vibration and asymmetrical stretching vibration for -OH near 3400 cm^{-1} and C-H near 2900 cm^{-1}, and the transmittance peak of double bonds stretching vibration for -C=O near 1700 cm^{-1} appeared on FTIR spectra of treated CNT. Compared to un-treated CNT

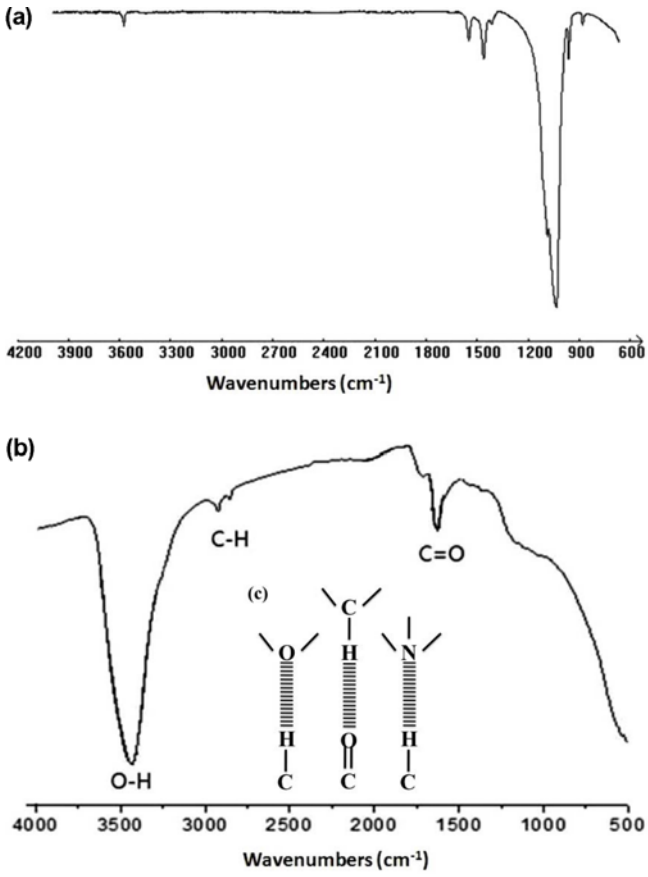

Fig. 6. FTIR spectra of (a) un-treated CNT and (b) treated CNT, and (c) hydrogen-bond-driven self-assembly.

with no chemical group, treated CNT had some active chemical groups, such as carboxyl and hydroxyl active groups on the surface. These active groups could undergo a hydrogen-bond-driven self-assembly[40,41] with the active groups in the matrix resin, as shown in Fig. 6(c).

On the basis of uni- and bi-modal ECAs, tri-modal ECAs (Table 3) were designed: the total electrically conductive filler content was 38 vol. %, the nano silver sphere content was 1 vol. %, and the treated CNT dispersed uniformly. As Figure 4(e) shows, the bulk resistivity decreased with the increase of treated CNT, and the minimum bulk resistivity was 2.9×10^{-5} Ω·cm at 0.5 vol. % of treated CNT, showing the treated CNT indeed improved the electrical conductivity. In tri-modal ECAs, the electrically conductive channels were formed by granular and linear electrically conductive fillers, which were different from that only formed by granular electrically conductive fillers in uni- and bi-modal ECAs. Tri-modal ECAs contained three different electrically conductive fillers: micron silver flakes, nano silver spheres, and treated CNT. The treated CNT played a role of linear electrically conductive filler to connect silver particles and form more electrically conductive channels.

As the treated CNT increased, the adhesion strength decreased linearly (Fig. 4(f)). In tri-modal ECAs, treated CNT only replaced a few micron silver flakes, but it brought significantly negative effect on the adhesion strength. The maximum adhesion strength was 10 MPa at 0.1 vol. % of treated CNT and the minimum adhesion strength of 5 MPa at 0.5 vol. % of treated CNT. In other words, treated CNT improved the electrical conductivity greatly, but also reduced the adhesion strength sharply. The reasons might be similar to that of bi-modal ECAs, but not exactly the same. For bi-modal ECAs, the decrease of adhesion strength was due to the great increase of solid-to-solid contact points brought by nano silver spheres. In tri-modal ECAs, linear CNT was not very straight and apparently many were bent. It gathered at the bonding interface. A lying CNT at the bonding interface brought a series of solid-to-solid contact points (Fig. 4(g)), not like a nano particle only brought a solid-to-solid contact point. These too many or series of solid-to-solid contact points reduced the adhesion strength of tri-modal ECAs greatly. Here, the bulk resistivity and adhesion strength were 3.5×10^{-5} Ω·cm and 10 MPa, respectively, for tri-modal ECAs at 36.9 vol. % of micron silver flakes, 1 vol. % of nano silver spheres, and 0.1 vol. % of treated CNT.

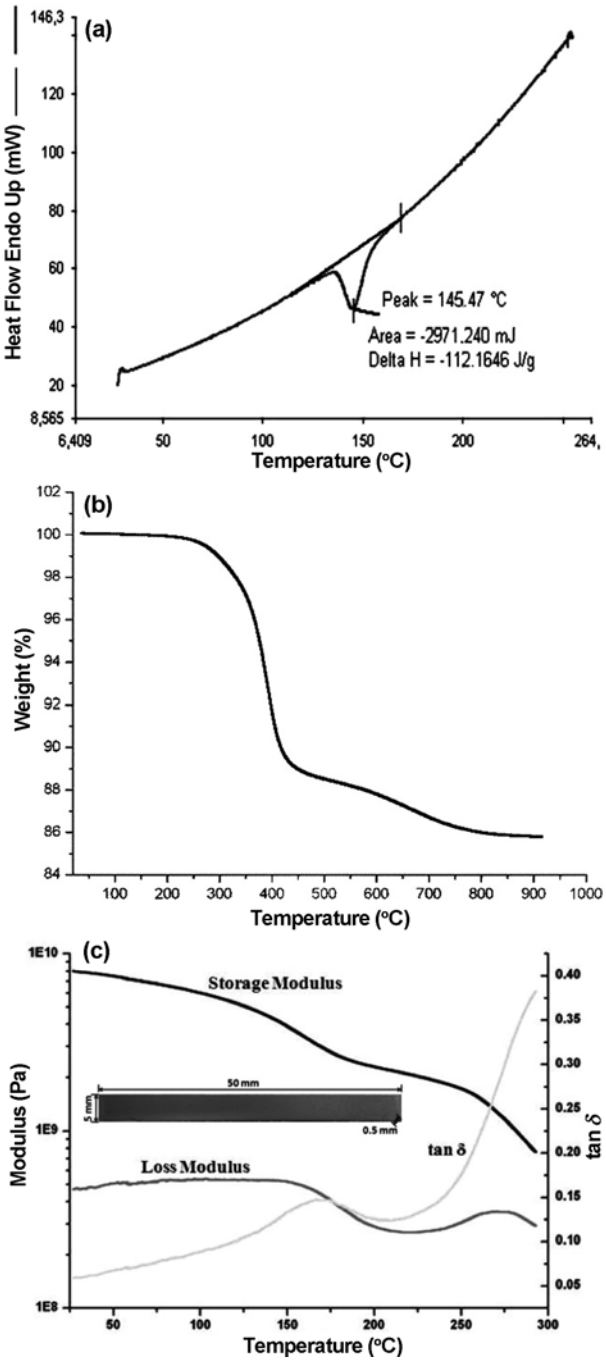

Fig. 7. (a) DSC, (b) TGA, and (c) tested sample and DMA curves of ECAs.

3.4 Thermal properties

The melt temperature of silver is very high. CNT's melt temperature is the highest in all the currently known materials.[42,43] Therefore, the thermal properties of ECAs are determined by the matrix resin completely, especially the curing, pyrolysis, and glass transition temperature. In this study, the matrix resin all was the same, containing a functional epoxy, a reactive diluent, a silane-coupling agent, and a curing agent. That is to say that the uni-, bi-, and tri-modal ECAs had similar or same thermal properties, so here, they were combined together to discuss, and the matrix resin was mainly used to investigate the thermal properties of ECAs.

As Figure 7(a) shows, ECAs started to cure at about 120°C, reached the peak at about 145°C, and almost finished

curing at about 170°C. The lowest curing temperature was 120°C. These ECAs could be cured at 120°C or any higher temperature than this with different curing time. The higher the curing temperature, the shorter the curing time. Figure 7(b) shows the pyrolysis process of ECAs. The weight began to lose at about 200°C, quickly lost from about 350°C to 400°C, and the pyrolysis rate in this range was the maximum. Above this temperature, the weight loss became slow. The pyrolysis temperature of ECAs was above 350°C. The storage modulus, loss modulus, and glass transition temperature of ECAs were not affected, either, as shown in Fig. 7(c). The glass transition temperature is defined as the temperature corresponding to the peak of tan δ. It was about 180°C, much higher than that of the currently used ECAs on the market around 80°C - 150°C.[44-46] These thermal properties showed the prepared uni-, bi-, and tri-modal ECAs all had high temperature stability.

4. CONCLUSIONS

In this study, a matrix resin containing a functional epoxy, a reactive diluent, a silane-coupling agent, and a curing agent was used to fabricate three modal ECAs with micron silver flakes, nano silver spheres, and treated CNT. These ECAs all were solvent-free. The bulk resistivity and adhesion strength of uni-modal ECAs were 5.0×10^{-5} Ω·cm and 15.2 MPa respectively at 38 vol. % of micron silver flakes. The lowest bulk resistivity of bi-modal ECAs was 3.9×10^{-5} Ω·cm, while the bulk resistivity and adhesion strength were 4.5×10^{-5} Ω·cm and 15 MPa respectively at 37 vol. % of micron silver flakes and 1 vol. % of nano silver spheres. The lowest bulk resistivity of tri-modal ECAs was 2.9×10^{-5} Ω·cm. When the contents of micron silver flakes, nano silver spheres, and treated CNT were 36.9 vol. %, 1 vol. %, and 0.1 vol. % respectively, the bulk resistivity was 3.5×10^{-5} Ω·cm and the adhesion strength was 10 MPa for tri-modal ECAs. The matrix resin determined the thermal properties of ECAs completely. The lowest curing temperature was 120°C, so they could be cured at 120°C or any higher temperature than this with different curing time. These ECAs all had high temperature stability with a pyrolysis temperature above 350°C and a glass transition temperature around 180°C.

ACKNOWLEDGEMENTS

This study was supported financially by Chinese Ministry of Science and Technology under 863 program (No. 2008AA04Z301), Chinese Ministry of Science and Technology for the International Science and Technology Cooperation Program of China (No. 2010DFA14450), Chinese Governmental 02 Special Program (No. 2011ZX02602), and Chinese Natinoal Science Foundation Project (No. 50876057).

REFERENCES

1. Y. Li and C. P. Wong, *Mater. Sci. Eng.* R **51**, 1 (2006).
2. I. Mir and D. Kumar, *Int. J. Adhes. Adhes.* **28**, 362 (2008).
3. F. Tan, X. Qiao, J. Chen, and H. Wang, *Int. J. Adhes. Adhes.* **26**, 406 (2006).
4. W. Lin, X. Xi, and C. Yu, *Synthetic Met.* **159**, 619 (2009).
5. Y. Zhang, S. Qi, X. Wu, and G. Duan, *Synthetic Met.* **161**, 516 (2011).
6. H. K. Kim and F. G. Shi, *Microelectron. J.* **32**, 315 (2001).
7. S. Xu and D. A. Dillard, *Int. J. Adhes. Adhes.* **23**, 235 (2003).
8. C. F. Goh, H. Yu, S. S. Yong, S. G. Mhaisalkar, F. Y. C. Boey, and P. S. Teo, *Thin Solid Films* **504**, 416 (2006).
9. Z. Wu, J. Li, D. Timmer, K. Lozano, and S. Bose, *Int. J. Adhes. Adhes.* **29**, 488 (2009).
10. Y. Guan, X. Chen, F. Li, and H. Gao, *Int. J. Adhes. Adhes.* **30**, 80 (2010).
11. R. S. Rörgren and J. Liu, *IEEE Trans. Compon. Pack. Manuf.* **18**, 305 (1995).
12. W.-K. Tao, S. Chen, X.-H. Liu, H.-W. Cui, T.-A. Chen, and J. Liu, *Proc. 2010 11th Int. Conf. Electron. Pack. Technol. High Density Pack*, p. 225, Xi'an, China (2010).
13. D.-S. Li, H.-W. Cui, S. Chen, Q. Fan, Z.-C. Yuan, L.-L. Ye, and J. Liu, *ECS Trans.* **34**, 583 (2011).
14. D.-S. Li, H.-W. Cui, Q. Fan, Y.-Y. Duan, Z.-C. Yuan, L.-L. Ye, and J. Liu, *Proc. 2011 12th Int. Conf. Electron. Pack. Technol. High Density Pack*, p. 430, Shanghai, China (2011).
15. W.-H. Du, H.-W. Cui, S. Chen, Z.-C. Yuan, L.-L. Ye, and J. Liu, *ECS Trans.* **34**, 805 (2011).
16. C. Khoo and J. Liu, *Circuit World* **22**, 9 (1996).
17. Y. Fu, J. Liu, and M. Willander, *Int. J. Adhes. Adhes.* **19**, 281 (1999).
18. Y. Fu, T. Wang, and J. Liu, *IEEE Trans. Compon. Pack. Manuf.* **26**, 193 (2003).
19. L. L. Ye, Z. H. Lai, J. Liu, and A. Thölén, *IEEE Trans. Compon. Pack. Manuf.* **22**, 299 (1999).
20. Y. Fu, M. Willander, and J. Liu, *J. Electron. Mater.* **30**, 866 (2001).
21. W.-H. Du, C.-E. Fu, S. Chen, H.-W. Cui, X.-H. Liu, T.-A. Chen, and J. Liu, *Proc. 2010 11th Int. Conf. Electron. Pack. Technol. High Density Pack*, p. 199, Xi'an, China (2010).
22. W.-H. Du, H.-W. Cui, S. Chen, Z.-C. Yuan, L.-L. Ye, and J. Liu, *Proc. 2011 12th Int. Conf. Electron. Pack. Technol. High Density Pack,* p. 1053, Shanghai, China (2011).
23. H.-X. Lai, X.-Z. Lu, H.-W. Cui, X.-H. Liu, S. Chen, T.-A. Chen, and J. Liu, *Proc. 2010 11th Int. Conf. Electron. Pack. Technol. High Density Pack*, p. 235, Xi'an, China (2010).
24. Q. Fan, H.-W. Cui, C.-E. Fu, D.-S. Li, X. Tang, Z.-C. Yuan, L.-L. Ye, and J. Liu, *ECS Trans.* **34**, 811 (2011).
25. Q. Fan, H.-W. Cui, D.-S. Li, Z.-L. Hu, Z.-C. Yuan, L.-L. Ye, and J. Liu, *Proc. 2011 12th Int. Conf. Electron. Pack.*

Technol. High Density Pack, p. 423, Shanghai, China (2011).
26. Z.-M. Mo, X.-T. Wang, T.-B. Wang, S.-M. Li, Z.-H. Lai, and J. Liu, *J. Electron. Mater.* **31**, 916 (2002).
27. M. Inoue, H. Muta, T. Maekawa, S. Yamanaka, and K. Suganuma, *J. Electron. Mater.* **37**, 462 (2008).
28. M. Inoue and J. Liu, *Proc. 2008 2nd Electron.s Systemintegration Technol. Conf,* p. 1147, Greenwich, CT, USA (2008).
29. E. Darque-Ceretti, D. Helary, and M. Aucoutier, *Glass Int.* **26**, 13 (2003).
30. S. G. Prolongo and A. Ureña, *Int. J. Adhes. Adhes.* **29**, 23 (2009).
31. J. J. Mock, M. Barbic, D. R. Smith, D. A. Schultz, and S. Schultz, *J. Chem. Phys.* **116**, 6755 (2002).
32. H.-H. Lee, K.-S. Chou, and Z.-W. Shih, *Int. J. Adhes. Adhes.* **25**, 437 (2005).
33. H. P. Wu, J. F. Liu, X. J. Wu, M. Y. Ge, Y. W. Wang, G. Q. Zhang, and J. Z. Jiang, *Int. J. Adhes. Adhes.* **26**, 617 (2006).
34. W. T. Cheng, Y. W. Chih, and W. T. Yeh, *Int. J. Adhes. Adhes.* **27**, 236 (2007).
35. Y. Fu, M. Willander, and J. Liu, *J. Electron. Mater.* **30**, 866 (2001).
36. S. Iijima, *Nature* **354**, 56 (1991).
37. W. E. Wong, P. E. Sheehan, and C. M. Liebert, *Science* **277**, 1971 (1997).
38. S. Kotthous, B. H. Günther, and R. Hang, *IEEE. Trans. Compon. Pack. Technol.* **20**, 15 (1997).
39. H. Zhao, X. Luo, and Y. Luo, *Chinese J. Appl. Chem.* **25**, 2630 (2008).
40. S.-W. Kuo, Y.-C. Chung, K.-U. Jeong, and F.-C. Chang, *J. Phys. Chem. C* **112**, 16470 (2008).
41. S.-W. Kuo and H.-T. Tsai, *Macromolecules* **42**, 4701 (2009).
42. G. E. Begtrup, K. G. Ray, B. M. Kessler, T. D. Yuzvinsky, H. Garcia, and A. Zettl, *Phys. Rev. Lett.* **99**, 155901 (2007).
43. K. Zhang, G. Malcolm Stocks, and J. Zhong, *Nanotechnology* **18**, 285703 (2007).
44. R. Zhang, K.-S. Moon, H. Jiang, W. Lin, and C. P. Wong, *Proc. PORTABLE-POLYTRONIC 2008 2nd IEEE Int. Interdisciplinary Conf. Portable Information Devices*, p. 1, Germany (2008).
45. Y. Li, K.-S. Moon, and C. P. Wong, US Patent: 7527749 (2009).
46. P. Mach, D. Busek, and R. Polansky, *Proc. 2010 3rd Electron. System-Integration Technol. Conf.,* p. 1, Berlin, Germany (2010).